Atom Indonesia

Journal homepage: http://aij.batan.go.id

Neural Network Predictions of Atomic Form Factors and Incoherent Scattering Functions

B. Mohammedi[1], H. Benkharfia[1], B. Beladel[2*], N. Mellel[1], K. Bessine[3], N. Moulai[4]

[1]*Nuclear Research Center of Birine, P.B.180, Ain Oussera 17200, Algeria*
[2]*Department of Physics, Ziane Achour University, Djelfa 17000, Algeria*
[3]*LDRSI Laboratory, Saad Dahlab University, Blida1, Blida 09000, Algeria*
[4]*Ecole Normale Superieure Kouba Algeirs, Algeria*

ARTICLE INFO

Article history:
Received 14 September 2022
Received in revised form 9 September 2023
Accepted 21 September 2023

Keywords:

Artificial neural networks
Atomic form factors
Incoherent scattering function
Compton total scattering cross sections

ABSTRACT

In order to predict atomic form factors and incoherent scattering functions which are used to calculate the coherent and incoherent total scattering cross sections, a technique based on artificial neural networks of the multilayer type was implemented. In this context, two neural models have been developed and compared with those in the literature. This study revealed both the accuracy of the results obtained and the effectiveness of the designed model. The mean relative error for the least estimated property does not exceed 16.5 %. The software realized in this way give a prediction of the above parameters for the input variables *Z*: Atomic number, *x*: sin(ϑ/2)/λ and *E*: Photon energy, and it provides users with flexibility for prediction. The advantages of this technique lie in its very fast handling, due to its ease of use, and in the two integrated networks, which it guarantees for a variety of input parameters such as atomic number, photon energy, and momentum transfer variable.

INTRODUCTION

The atomic form factor is defined as a measure of the scattering amplitude of an incident wave by an isolated atom. The atomic form factor, or atomic scattering factor for the photon-atom interaction is a complex number whose modulus represents the number of electrons in the atom participating in the scattering of the incident radiation in the direction of angle 2θ with the incident beam. The scattering of a radiation is coherent if the scattered photon fully retains its initial energy, leaving the scattered electron in its original state; otherwise, it is incoherent, in this case: the electron of the atom changes state and the scattered photon loses a part of its initial energy. These two processes take place simultaneously. The incoherent scattering function $S(x,Z)$, where x is a pulse transfer variable depending on the energy of the incident photons in addition to the deflection angle of the scattered photons and Z is the atomic number, is used for the treatment of deviations, with respect to Klein-Nishina expressions, of real atoms. This incoherent scattering function is also included in the cross section calculations for the production of electron-positron pairs in atomic electron fields, also known as the production of triplets [1-2].

Based on theoretical data, Hubbell [1] presented in his paper a tabulation for atomic form factors $F(x,Z)$, and the incoherent scattering functions, $S(x,Z)$ for values of x (=sin ϑ/2)/λ) from 0.005 Å^{-1} to 109 Å^{-1}, for all elements Z=1 to 100. With this data, he calculated Rayleigh and Compton total scattering cross sections for photon energies 100 eV to 100 MeV [1].

Since then, and given the great significance of coherent and incoherent total scattering cross sections in the calculation of radiation attenuation, reactor shielding, industrial radiography, medical physics, in addition of variety of other applications, several works have been carried out to improve the determination of these parameters, among them is ENDF/B-VIII.0.

ENDF/B-VIII.0 being the 8th major edition of the nuclear reactions data library of the pilot project of the international coordination of the CIELO evaluation library. The assessments benefit from recent experimental data obtained in Europe and the United States in addition to improvements in theory and simulation [3].

*Corresponding author.
E-mail address: b.beladel@univ-djelfa.dz
DOI: https://doi.org/10.55981/aij.2023.1275

In this trajectory of refining essential scattering parameters, a significant evolution has transpired through the infusion of artificial intelligence, particularly through the integration of neural networks. As a result, this study embarks on a novel task to explore the incorporation of neural networks for the improved prediction of atomic form factors and incoherent scattering functions.

METHODOLOGY

A neural network is a black box model which does not require any detailed information on the system. It is an advanced mathematical modeling procedure inspired by the biological neural system. The approach seems perfectly suited to problems where the relationships between variables are not linear and complex. In the structure of multilayer neural networks, neurons are grouped into layers, an input neuron layer, an output neuron layer, and one or more hidden layers which are made up of many interconnected neurons with a sigmoid activation function [4].

The elaboration of a database is a crucial phase of neural model designing. The selection of inputs consists of determining the relevant variables about the quantity to be modeled. It aims at two main points: the reduction of the dimension of the variables representation space of the model and the elimination of the inputs which have little or no influence on the output.

To build a reliable and representative database, a methodology is followed which include: inputs selection of neural model, data collection of data formatting, and data normalization. Based on this global strategy, details of the different phases of the procedure to follow are depicted in Fig. 1 [5].

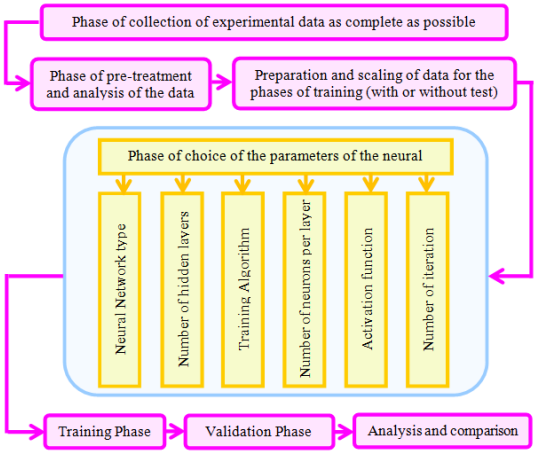

Fig. 1. Procedure for neural network modeling.

Each step mentioned in the flowchart presented in Fig. 1 is elaborated below.

The design of a neural model consists of carrying out an evaluation study of the constituent elements of the network according to the desired performance of the modeling. The aim of this study is to build two Artificial Neural Network models, ANN1 and ANN2. The first network is capable of predicting the atomic form factor and the incoherent diffusion function, the second network is for the coherent and incoherent scattering cross section predicting.

It is therefore a question of doing static modeling; the adequate network in view of the monograph consulted can generally only be a Multi Layer Perceptron (MLP) feed-forward network type. The most useful form of the neural model is the linear combination of nonlinear functions parameterized variables [6].

Normalization of values is a crucial step in the design of artificial neural networks, as sigmoid type bounded transfer functions are often used in static models. Almost the values of the neural network input differed by several orders of magnitude, which may not reflect the relative importance of the inputs determining the desired parameter at the output. For this purpose, the input and output data were normalized in the range of [-1,1] using a double normalization, the logarithmic function and the mapminmax algorithm given by Eq. 1, which performs a normalization of the maximum and minimum value of each row [4].

$$y_n = \frac{2(x - x_{min})}{(x_{max} - x_{min})} - 1 \qquad (1)$$

where x is the original vector value, x_{max} and x_{min} are the maximum and minimum values corresponding to x, respectively, and y_n is the vector value normalized by the vector x.

After reviewing a considerable number of neural networks, differently structured, the adequate artificial neural networks selected in this investigation, for each network, three hidden layers with 40 neurons each and an output layer with two neurons. Also for each network, the hidden layers have a tansig transfer function and the output layer has a linear transfer function. For the first network, two variables, Z: Atomic number and x: (=sin $\vartheta/2)/\lambda$) were introduced at the input while $F(x,Z)$: atomic form factor and $S(x,Z)$: the incoherent scattering function are introduced as output variables. For the second network, the two input variables are Z: Atomic number and E: Photon energy and the output variables are σ_{Coh}: coherent scattering cross section and σ_{Inc}: incoherent scattering cross section. Figure 2 shows the typical structure of an artificial neural network for the second neural network ANN2 [1,3,7].

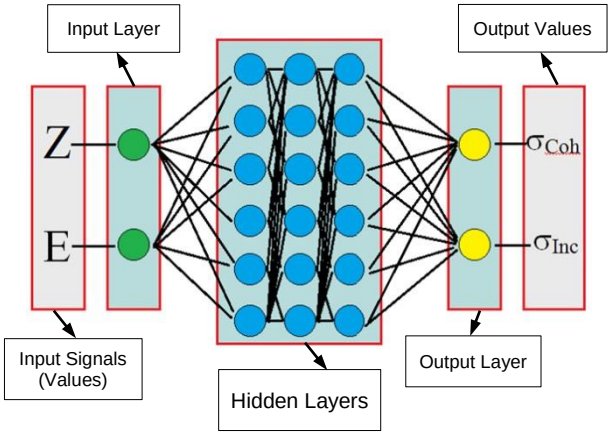

Fig. 2. Structural diagram of the ANN model.

The number of experimental data used, respectively, in ANN1 and ANN2 is 22987 and 24438. The two databases are divided into three sections: for the ANN1, the training set (19215 data), i.e. 83.60 % of the experimental database, the test set (1885 data) and the validation set (1887 data), i.e. 8.20 % for each set and for the ANN2, the training set (19700 data), nearly 80.60 % of the experimental database, the test set (2360 data) and the validation set (2378 data), that is to say 9.70 % for each set. Table 1 shows the range of variables for each network [1,7].

Table 1. Variables range.

Parameter	Measure	Unit	Min	Max
ANN1				
Input				
Atomic Number	Z	-	1.00E00	1.00E02
Sin(Theta/2)/Lambda	x	-	0.00E00	1.00E09
Output				
Atomic Form Factor	$F(x,Z)$	-	8.18E-39	1.00E02
Incoherent Scattering Function	$S(x,Z)$	-	0.00E00	1.00E02
ANN2				
Input				
Atomic Number	Z	-	1.00E00	1.00E02
Photon Energy	E	eV	1.00E00	1.00E11
Output				
Coherent Scattering Cross-Section	σ_{Coh}	Barns/atom	4.63E-16	3.44E04
Incoherent Scattering Cross-Section	σ_{Inc}	Barns/atom	7.17E-08	4.09E01

Performance assessment

For the statistical study and in order to measure the performance of neural network models, ANN1 and ANN2, developed for the prediction of four physical parameters, several performance criteria were used. Mean Relative Absolute Error (*MRAE*), Root Mean Squared Error (*RMSE*), Correlation Coefficient (*R*), Coefficient of Determination (R^2), Accuracy Factor (A_f), Bias Factor (B_f), Wilmot's index (*WI*), Legates-McCabe's index (*LMI*) and the acceptability criteria (*K*) and (*K'*) were used as a measure of precision and expressed as follows [8-14]:

- Mean Relative Absolute Error:

$$MRAE(\%) = \left[\frac{1}{n}\sum_{i=1}^{n}\frac{|y^{exp} - y^{pre}|}{y^{exp}}\right] * 100 \quad (2)$$

- Root Mean Square Error:

$$RMSE = \left[\frac{1}{n}\sum_{i=1}^{n}(y^{exp} - y^{pre})^2\right]^{1/2} \quad (3)$$

- Correlation Coefficient:

$$R = \frac{\sum_{i=1}^{n}\left(y_i^{pre} - \overline{y^{pre}}\right)\left(y_i^{exp} - \overline{y^{exp}}\right)}{\left[\sum_{i=1}^{n}\left(y_i^{pre} - \overline{y^{pre}}\right)^2 \sum_{i=1}^{n}\left(y_i^{exp} - \overline{y^{exp}}\right)^2\right]^{1/2}} \quad (4)$$

- Coefficient of Determination:

$$R^2 = 1 - \frac{\sum_{i=1}^{n}\left(y_i^{exp} - y_i^{pre}\right)^2}{\sum_{i=1}^{n}\left(y_i^{exp} - \overline{y_i^{exp}}\right)^2} \quad (5)$$

- Accuracy Factor:

$$A_f = 10^{\left[\frac{1}{n}\Sigma_1^n\left|log\frac{y_i^{pre}}{y_i^{exp}}\right|\right]} \quad (6)$$

- Bias Factor:

$$B_f = 10^{\left[\frac{1}{n}\Sigma_1^n log\frac{y_i^{pre}}{y_i^{exp}}\right]} \quad (7)$$

- Wilmot's Index:

$$WI = 1 - \frac{\sum_{i=1}^{n}(y^{exp} - y^{pre})^2}{\sum_{i=1}^{n}\left[\left|y_i^{pre} - \overline{y_i^{exp}}\right| + \left|y_i^{exp} - \overline{y_i^{exp}}\right|\right]^2} \quad (8)$$

- Legates-McCabe's Index:

$$LMI = 1 - \frac{\sum_{i=1}^{n}|y^{exp} - y^{pre}|}{\sum_{i=1}^{n}|y^{exp} - \overline{y^{exp}}|} \quad (9)$$

- Criteria of acceptability:

$$k = \frac{\sum_{i=1}^{n} y_i^{pre} y_i^{exp}}{\sum_{i=1}^{n} y_i^{pre\,2}} \quad (10)$$

- Criteria of acceptability:

$$k' = \frac{\sum_{i=1}^{n} y_i^{pre} y_i^{exp}}{\sum_{i=1}^{n} y_i^{exp\,2}} \quad (11)$$

RESULTS AND DISCUSSION

By applying Eq. 2 to Eq. 11 above, Table 2 and Table 3 below compile some static performances of the network parameters of the ANN1 and ANN2, of the design phase of the neural model, that is to say, training, testing, validation phase and the entire database.

For the sake a better presentation of the results, those obtained during the training and validation phases of the neural model design phase are presented first. Table 2, Fig. 3 and Fig. 4 present the results for the ANN1. For example, the results relating to the atomic form factor $F(x,Z)$, in the testing phase are noted, the Mean Relative Absolute Error value against the dataset is less than 0.38 % and it is less than 1.85 % for the incoherent scattering function $S(x, Z)$, also in the testing phase. The correlation coefficient value of 1 for all data indicated the reliability of the ANN1 model.

For ANN1, the accuracy factor A_f and the bias factor B_f, which are criteria for evaluating the performance of the model, are equal to unity. Indeed, the precision factor A_f will always be one or greater than one because all the variances are positive. The A_f value of 1.1 means that the predicted value is 10 % different from the experimental value. The B_f indicates the overall agreement between the predicted values and the experimental values, a B_f equal to 1 signifies a total agreement. For a B_f = 0.9-1.05, the model is good; for a B_f between 0.7 and 0.9, the model is acceptable. The model is to be used with caution for a B_f between 1.06 and 1.15, and for a B_f <0.7 and B_f > 1.14, the model is rejected.

Two other indices measure precision: the Wilmot index and the Legates-McCabe index, whose values are practically equal to 1.

The ANN1 model was also evaluated by the acceptability criteria K and K' which are equal to 1, our model is acceptable because $0.85 \leq K \leq 1.15$ and $0.85 \leq K' \leq 1.15$. It is important to note that the size of the matrices used to perform the training is 19215, the validation of 1887 and for the test of 1885 columns.

Table 2. Performance metrics of the ANN1.

Performance	Function	Training	Testing	Validation	All
MRAE%	$F(x,Z)$:	332.0473e-03	378.3296e-03	359.1478e-3	338.0673e-03
	$S(x,Z)$:	1.3722e00	1.8509e00	1.8155e00	1.4478e00
MSE	$F(x,Z)$:	1.5957e-03	3.3917e-03	3.4347e-03	1.8940e-03
	$S(x,Z)$:	18.2623e-03	25.2280e-03	25.1862e-03	19.4019e-03
R	$F(x,Z)$:	999.9976e-03	999.9959e-03	999.9957e-03	999.9973e-03
	$S(x,Z)$:	999.9823e-03	999.9742e-03	999.9744e-03	999.9811e-03
R^2	$F(x,Z)$:	999.9952e-03	999.9916e-03	999.9914e-03	999.9946e-03
	$S(x,Z)$:	999.9647e-03	999.9483e-03	999.9487e-03	999.9623e-03
A_f	$F(x,Z)$:	1.0000e00	1.0000e00	1.0000e00	1.0000e00
	$S(x,Z)$:	1.0000e00	1.0000e00	1.0000e00	1.0000e00
B_f	$F(x,Z)$:	1.0000e00	999.9995e-03	1.0000e00	1.0000e00
	$S(x,Z)$:	999.9993e-03	999.9995e-03	999.9994e-03	999.9993e-03
WI	$F(x,Z)$:	999.9988e-03	999.9979e-03	999.9978e-03	999.9986e-03
	$S(x,Z)$:	999.9912e-03	999.9871e-03	999.9872e-03	999.9906e-03
LMI	$F(x,Z)$:	998.8551e-03	998.3931e-03	998.4045e-03	998.7763e-03
	$S(x,Z)$:	995.9505e-03	995.1996e-03	995.2054e-03	995.8444e-03
K	$F(x,Z)$:	1.0001e00	1.0002e00	1.0002e00	1.0001e00
	$S(x,Z)$:	999.9772e-3	1.0000e00	1.0000e00	999.9829e-03
K'	$F(x,Z)$:	999.8797e-3	999.7696e-03	999.8339e-03	999.8630e-03
	$S(x,Z)$:	1.0000e00	999.9650e-03	999.9465e-03	1.0000e00
Best linear fit	$F(x,Z)$:	Y=T+0.00046	Y=T-0.002	Y=T+0.0027	Y=T+0.00044
	$S(x,Z)$:	Y=T+0.00034	Y=T+0.014	Y=T+0.014	Y=T+0.0029

Table 3. Performance metrics of the ANN2.

Performance	Function	Training	Testing	Validation	All
MRAE%	σ_{Coh}	2.9470	2.1122	2.1387	2.7877
	σ_{Inc}	927.5628E-3	831.7655E-3	844.6996E-3	910.2484E-3
MSE	σ_{Coh}	226.2057	230.0990	230.4619	226.9958
	σ_{Inc}	1.1026E-3	1.8322E-3	1.8366E-3	1.2445E-3
R	σ_{Coh}	999.4291E-3	999.4836E-3	999.4779E-3	999.4415E-3
	σ_{Inc}	999.9851E-3	999.9808E-3	999.9808E-3	999.9845E-3
R^2	σ_{Coh}	998.8458E-3	998.9646E-3	998.9541E-3	998.8737R-3
	σ_{Inc}	999.9703E-3	999.9616E-3	999.9616E-3	999.9690E-3
A_f	σ_{Coh}	1.0000	1.0000	1.0000	1.0000
	σ_{Inc}	1.0001	1.0001	1.0001	1.0001
B_f	σ_{Coh}	1.0000	1.0000	1.0000	1.0000
	σ_{Inc}	1.0000	1.0000	1.0000	1.0000
WI	σ_{Coh}	999.7102E-3	999.7406E-3	999.7380E-3	999.7173E-3
	σ_{Inc}	999.9926 E-3	999.9904E-3	999.9901E-3	999.9922E-3
LMI	σ_{Coh}	980.4174E-3	981.8240E-3	981.7806E-3	980.8198E-3
	σ_{Inc}	996.6802 E-3	995.5050E-3	995.5334E-3	996.4991E-3
K	σ_{Coh}	1.0031	1.0015	1.0012	1.0027
	σ_{Inc}	1.0000	999.8775E-3	999.9243E-3	999.9768E-3
K'	σ_{Coh}	995.8989E-3	997.6942E-3	997.9403E-3	996.3370E-3
	σ_{Inc}	999.9704 E-3	1.0001	1.0001	1.0000
Best linear fit	σ_{Coh}	Y=T+1.1	Y=T+0.19	Y=T+0.27	Y=T+0.92
	σ_{Inc}	Y=T+0.00011	Y=T-0.00035	Y=T-0.0002	Y=T+4.9E-5

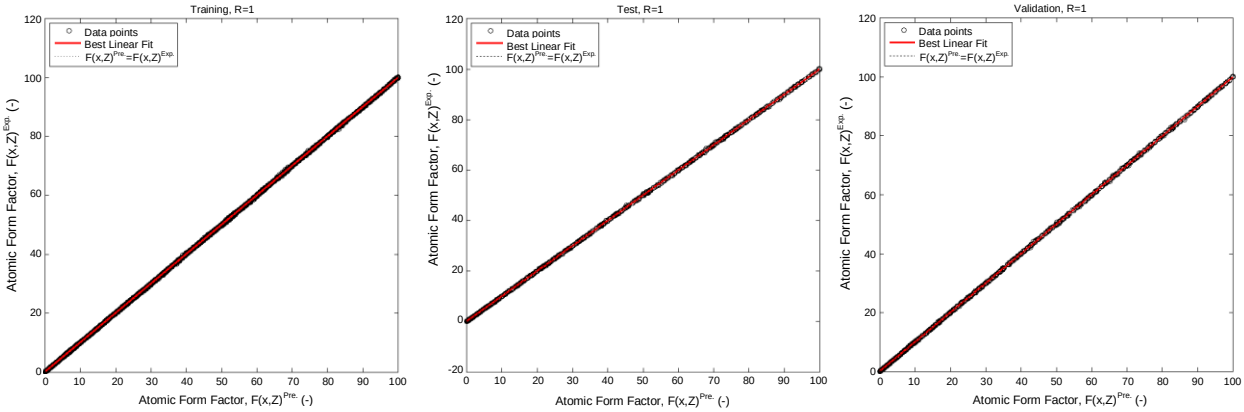

Fig. 3. Regression plots of the ANN model for the prediction of the atomic form factor, $F(x, Z)$.

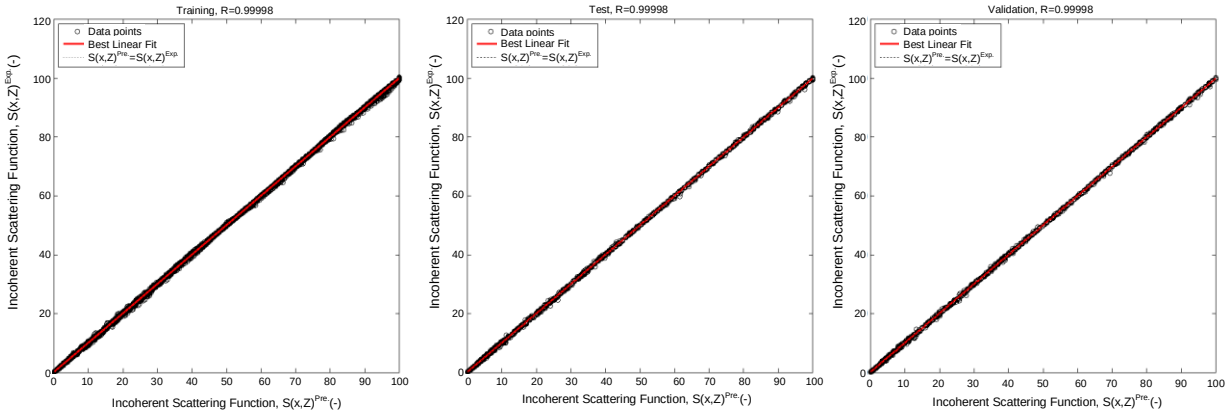

Fig. 4. Regression plots of the ANN model for the prediction of the incoherent scattering function, $S(x, Z)$.

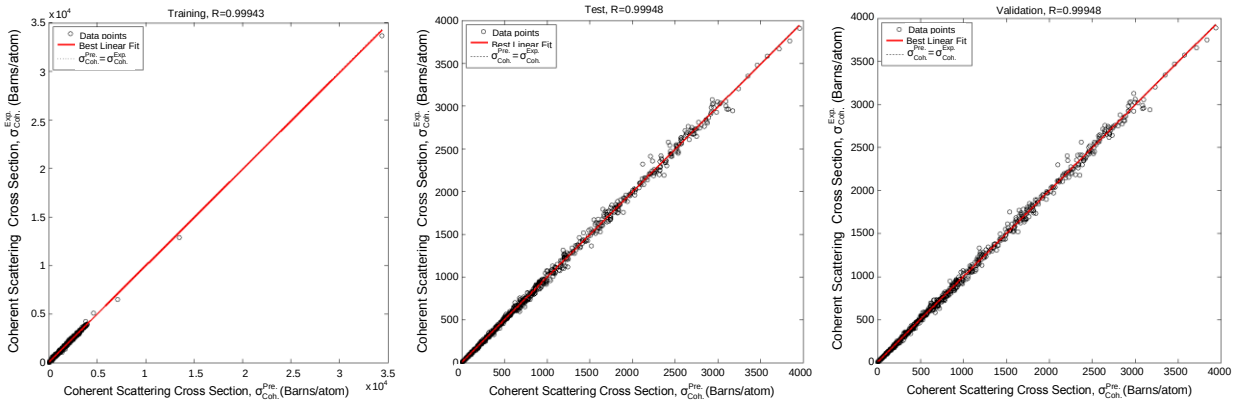

Fig. 5. Regression plots of the ANN model for the prediction of the coherent scattering cross-section, $\sigma_{Coh.}$

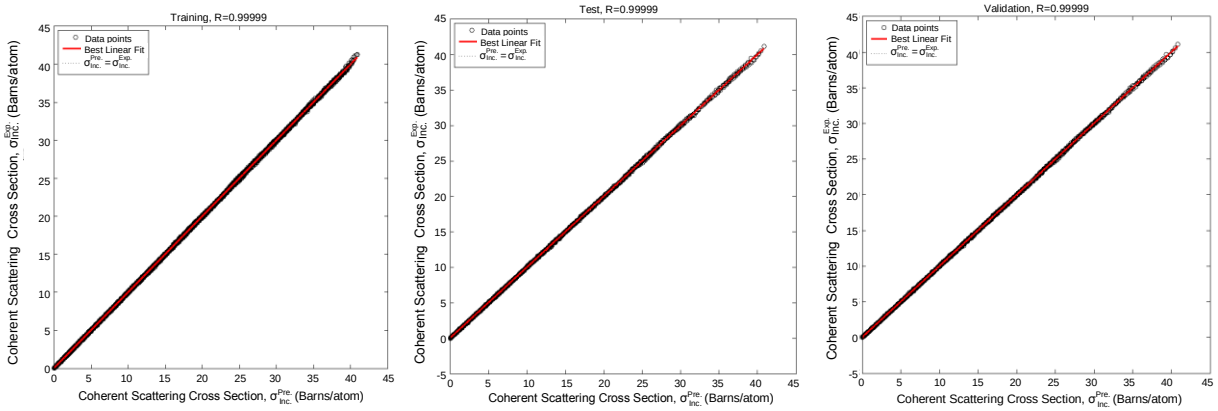

Fig. 6. Regression plots of the ANN model for the prediction of the incoherent scattering cross-section, $\sigma_{Inc.}$

Table 3, Fig. 5 and Fig. 6 show the results of the ANN2 network, for example, the coherent scattering cross-section σ_{Coh}, in the training phase, Mean Relative Absolute Error value with respect to the dataset is less than 2.95 % and less than 0.93 % for the incoherent scattering cross-section σ_{inc}, also in the training phase. The correlation coefficient R is equal to 1.

For ANN2, the accuracy factor A_f and the bias factor B_f, are also equal to 1, indicating full agreement. The ANN2 model is also acceptable because K and K' are equal to 1. And for the precision, the Wilmot's index and the Legates-McCabe index, their values are practically equal to 1. It is important to mention that the size of the matrices used to perform the training is 19700, the validation is 2378, and for the test 2360 columns.

It is important to note that the two neural models ANN1 and ANN2 perfectly reproduce the experimental data that were used for training and validation. The two networks manage to keep up with the evolution of the output parameters which puts them out of the domains of under or overfitting. It is clear that the distribution of the predicted results, of the two neural models, around the experimental values is quite acceptable; the Mean Relative Absolute Error committed on this sample is less than 2 %.

To measure the performance of the designed neural models, the results obtained are compared with those of the models proposed by ENDF/B-VIII.0 [7]. Table 4 presents the comparative study between the neural model and ENDF/B-VIII.0 for the four parameters of the two networks ANN1 and ANN2. The obtained results, as can be seen, are in complete agreement with the model of ENDF/B-VIII.0. The average relative error made over the whole of this test oscillates between 0.16 % for the incoherent scattering function $S(x,Z)$ of the ANN1 network and 0.74 % for the coherent scattering cross-section σ_{coh} of the ANN2 network.

Another comparison study was carried out by comparing the predictions of the ANN2 neural network with the results taken from Hubbell et al. [1], which has long been a reference in this field.

According to Table 5 above, a large deviation of the coherent scattering cross-section σ_{coh} is observed compared to the the reference [1]. Indeed, the average relative error is 335.56 %, while the error values vary between 15.57 % and 945.11 %. On the other hand, for the network ANN2, the mean relative error of the coherent diffusion cross-section is 3.72 %.

Table 4. Comparative study between the neural model and the ENDF/B-VIII.0.

				ENDF/B-VIII.0[2]	**Neural model**	
ANN1	**Element**	**Z[-]**	**x[-]**	**Value**	**Value**	**RE [%]**
$F(x,Z)$	H	1	2.00e-02	9.9121e-01	9.8990e-01	0.32
[-]	Mn	25	1.50e-01	2.0739e+01	2.0837e+01	0.49
	Sn	50	7.00e+00	1.3552e+00	1.3660e+00	1.07
	Re	75	5.00e+01	1.1445e-01	1.1397e-01	0.18
	Ra	88	1.00e+03	9.2072e-05	9.2163e-05	0.30
MRE						**0.47**
$S(x,Z)$	P	15	3.00e-02	2.7660e-01	2.9489e-01	0.20
[-]	Br	35	7.00e-01	1.8185e+01	1.8043e+01	0.78
	Nd	60	1.25e+00	3.7848e+01	3.7789e+01	1.60
	At	85	1.00e+02	8.5000e+01	8.5000e+01	0.00
	Fm	100	1.00e+06	1.0000e+02	1.0000e+02	0.00
MRE						**0.16**
ANN2	**Element**	**Z[-]**	**E[ev]**	**Value**	**Value**	**ER [%]**
σ_{Coh}	N	7	4.00e+02	8.6172e-01	8.5945e-01	0.26
[Barns/Atom]	V	23	8.00e+03	1.1012e+02	1.1123e+02	1.01
	Sm	62	6.00e+05	1.1894e+00	1.1943e+00	0.41
	Rn	86	5.00e+06	4.2739e-02	4.2406e-02	0.78
	Es	99	5.00e+07	6.4080e-04	6.3279e-04	1.25
MRE						**0.74**
σ_{Inc}	Li	3	1.00e+03	3.5514e-01	3.5322e-01	0.54
[Barns/Atom]	K	19	3.00e+04	9.1651e+00	9.1615e+00	0.04
	Mo	42	8.00e+05	9.8111e+00	9.8147e+00	0.04
	Lu	71	6.00e+06	5.1963e+00	5.1742e+00	0.43
	Cf	98	4.00e+07	1.7115e+00	1.7048e+00	0.39
MRE						**0.29**

[2]By interpolation specific to NDF evaluation

Table 5. Comparative study between ANN2 and the Hubbell model J.H compared to the ENDF/B-VIII.0.

				ENDF/B-VIII.0[3]	Hubbell J.H		Neural model	
ANN2	**Element**	**Z[-]**	**E[ev]**	**Value**	**Value**	**RE [%]**	**Value**	**RE [%]**
σ_{Coh} [Barns / Atom]	C	6	1.00e+02	9.4818e+00	2.3940e+01	152.48	1.0241e+01	8.01
			1.50e+02	8.4347e+00	2.3900e+01	183.35	8.6939e+00	3.07
			1.00e+03	2.5549e+01	2.1570e+01	015.57	2.5727e+01	0.70
	Sn	50	1.00e+02	3.4238e+02	1.6620e+03	385.43	3.3376e+02	2.52
			1.50e+02	1.5893e+02	1.6610e+03	945.11	1.5532e+02	2.27
			1.00e+03	1.3166e+03	1.5740e+03	019.55	1.3520e+03	2.69
	Fm	100	1.00e+02	9.69113e+02	6.6490e+03	586.09	1.0230e+03	5.56
			1.50e+02	9.57275e+02	6.6440e+03	585.58	9.2975e+02	2.88
			1.00e+03	2.57905e+03	6.3680e+03	146.91	2.7276e+03	5.76
MRE						**335.56**		**3.72**

[3]By interpolation specific to NDF evaluation

Software organization chart

Among the most obvious applications of neural networks are prediction applications, in our case the prediction of the atomic form factor, the incoherent scattering function, the coherent scattering cross-section and the incoherent scattering cross-section $F(x,Z)$, $S(x,Z)$, σ_{Coh} and σ_{Inc}, respectively. This type of applications is of great importance to people who have to perform calculations that, in the absence of powerful software, can be often complex and time-consuming.

Traditionally, the user has had to familiarize themselves with the use of tabulations constructed from theoretical data. The use of these tables gives rise to more tedious computation, often very repetitive, which distract from the principal.

In fulfilling this real expectation, we have integrated the two neural networks ANN1 and ANN2, already validated, that is to say, the weights and biases of each layer are determined, in a program to make precise complex calculations very easily and in a minimum time period. This program can rigorously predict the atomic form factor, the incoherent scattering function, the coherent scattering cross-section and the incoherent scattering cross-section of all elements from Z = 1 to Z = 100 using equation (12) below [4,14].

$$g(x,w) = \sum_{i=1}^{N_h} \left[w_{N_h+1,i}\, th\left(\sum_{j=1}^{n} w_{ij} x_j + b_i \right) + b_{N_h} \right] \quad (12)$$

where $g(x,w)$ is the output, w and b are respectively the weight and the bias, N_h and n are respectively the number of the hidden layers and the number of neuron; x is normalized input, and th is transfer function.

Figure 7 shows the designed software interface in a user-friendly way [15,16]. On the left is displayed all the chemical elements of the Mendeleev table ordered by increasing atomic number and organized according to their electronic configuration. On the top right of the window are displayed the chemical properties of the elements including the atomic number which is the first entry and common for both networks. On the lower part of the window are two tabs one for $\sin(\vartheta/2)/\lambda$ where introduces this value, as the second input parameter of the first neural network ANN1, to obtain the atomic form factor and of the incoherent scattering function and the other for photon energy where this value is introduced, as the second input parameter of the second neural network ANN2, to obtain the coherent and the incoherent scattering cross-section.

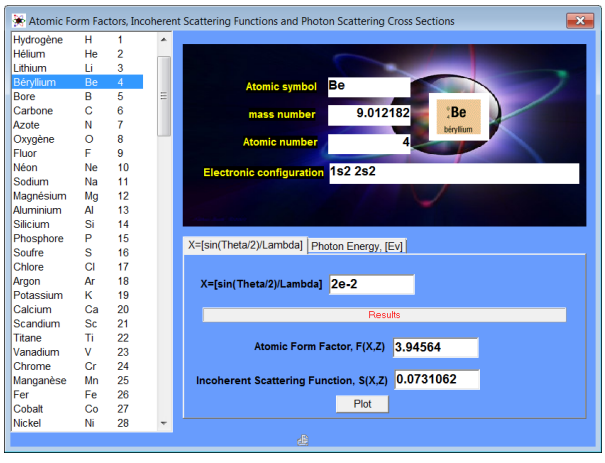

Fig. 7. Soft interface for predicting the $F(x,Z)$, $S(x,Z)$, σ_{Coh} and σ_{Inc} using Artificial Neural network.

Figure 8 shows an example of output from the software.I It presents the plot of the coherent scattering cross-section, σ_{Coh} of Fermium element whose atomic number Z=100, where x=sin(ϑ/2)/λ varied from 0 to 1000 by a step of 10.

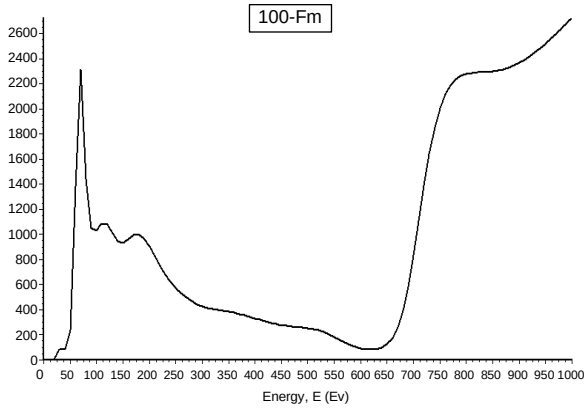

Fig. 8. Plot of coherent scattering cross-section, σ_{Coh} of Fermium element.

CONCLUSION

The development of applications involving artificial neural networks in the calculations and prediction of atomic form factors, incoherent scattering functions in addition to coherent and incoherent scattering cross sections $F(x,Z)$, $S(x,Z)$, σ_{Coh} and σ_{Inc}, respectively, proves to be beneficial. The advantage of this method is highlighted by its inclusion the good agreement, when comparing the results obtained by neural networks and referring to both previous works from international bibliographic database and experience. Errors, likely to be made remain very acceptable; indeed, the comparative studies carried out during the comparison of the results show their effectiveness and their performances. Hence, it is concluded the neural models developed in this work are reliable and efficient tools and can be successfully employed to provide an accurate prediction of the form factors and scattering cross sections. The integration of these models in a computer program will allow users, for complex calculations, their application with simplicity and speed in a minimum of time.

ACKNOWLEDGEMENT

This work was supported by the Algerian Atomic Energy Commission. The authors are grateful for the financial support.

REFERENCES

1. J. H. Hubbell, Wm. J. Veigele, E. A. Briggs *et al.*, J. Phys. Chem. Ref. Data **4** (1975) 471.
2. M. Herman and A. Trkov, ENDF-6 Formats Manual: Data Formats and Procedures for the Evaluated Nuclear Data Files. National Nuclear Data Center, Brookhaven National Laboratory, Upton, NY 11973-5000 (2010).
3. D. A. Brown, M. B. Chadwick, R. Capote *et al*., Nucl. Data Sheets **148 (**2018) 1.
4. H. Demuth and M. Beale, Neural Network Toolbox User's Guide. The MathWorks, Inc (2009).
5. C. Si-Moussa, S. Hanini, R. Derriche *et al*., Braz. J. Chem. Eng. **25** (2008) 183.
6. B. Beladel, B. Mohamedi, A. Guesmia *et al*., Radiochim. Acta **106** (2018) 1017.
7. D. E. Cullen, M. H. Chen, J. H. Hubbell *et al*., The Livermore Evaluated Photon Data Library (EPDL97) in the ENDF-6 Format. International Atomic Energy Agency, Vienna, Austria (2018). https://www-nds.iaea.org/public/download-endf/ENDF-B-VIII.0/photo/
8. A. Golbraikh and A. Tropsha, J. Mol. Graph. Model. **20** (2002) 269.
9. A. Bouali, S. Hanini, B. Mohammedi *et al*., Therm. Sci. **25** (2021) 3911.
10. A. Bouzidi, S. Hanini, F. Souahi *et al*., J Appl Sci. **7** (2007) 2450.
11. H. Sanikhani, R. C. Deo, Z. M. Yaseen *et al*., Geoderma **330** (2018) 52.
12. S. Y. Park, S. Y. Choi and S. D. Ha, Foodborne Pathog Dis. **16** (2019) 376.
13. T. Ross, J. Appl.Bacteriol. **81** (1996) 501.
14. D. G. Garson, AI Expert. **6** (1991) 47.
15. Sigma, Evaluated Nuclear Data File (ENDF) Retrieval & Plotting, National Nuclear Data Center, Brookhaven National Laboratory, NY (2011).
16. B. Pritychenko and A. A. Sonzogni, Nucl. Data Sheets. **109** (2008) 2822.